

MULTIRESOLUTION METRICS FOR DETECTING SINGLE-TRIAL EVOKED RESPONSE POTENTIALS (ERPS)

TERRY A. LORING¹, DAVID E. WORTH², AKAYSHA C. TANG³

^{1,2}Department of Mathematics and Statistics, University of New Mexico, Albuquerque, New Mexico 87131, USA

³Department of Psychology, Department of Neurosciences, and Department of Computer Science,
University of New Mexico, Albuquerque, New Mexico 87131, USA

E-MAIL: loring@math.unm.edu, cesium@unm.edu, akaysha@unm.edu

Abstract:

It is desirable to determine from electroencephalography (EEG) or magnetoencephalography (MEG) the time course of brain activation in response to sensory stimulation. Because of the relatively poor signal to noise ratio, evoked responses potentials (ERPs) were typically measured by averaging over multiple trials. While recent applications of blind source separation (BSS) and independent component analysis (ICA) improved the effective signal to noise ratio (S/N) by separating different brain sources and other extra-cranial sources, variations in the background on-going activity of each brain source makes it difficult to determine whether and when an evoked response potential has occurred.

We introduced and combined several new approaches to improve single-trial ERP detection from a previously reported MEG data set with relatively low S/N. First, new metrics based on multiresolution filtering were introduced to better discriminate a ERP against background oscillatory activity. Second, a novel interactive user interface was implemented to use the new metrics to detect single-trial ERPs from an example. Third, time series of brain source activation recovered using BSS were used as inputs to this multiresolution method. We report sharpened average ERPs after alignment using the detected single-trial ERP onset time and a reduction in false detection from the previously reported 26+/-2% to 13+/-2%.

Keywords:

Multiresolution; metric; BSS; SOBI; MEG; onset; ERP; single-trial.

1. Introduction

1.1. Multiresolution methods

Wavelets are an attractive method for the analysis of time series as they break down information according to scale without losing too much position information. However, the two variations on the wavelet transform ([13]), the continuous and the discrete, each have drawbacks. The continuous transform is

expensive to compute, and outputs a lot of information for further processing. The discrete transform can be calculated quickly and has more limited output. Its disadvantage is that its filters operate at scales fixed at powers of two, which may not be optimal. Also, it is not even approximately shift invariant, as is pointed out in [7].

We introduce a multiresolution filtering method that is a compromise between the continuous and the discrete wavelet transform. It has filters that are approximately shift invariant, and the scales at which the filters operate can be set to match the features of a particular data set. The resulting filterbanks are one-dimensional analogs of filterbanks used in image analysis [7].

Suppose an expert has selected a time value that reflects a particular feature in the time series, such as an ERP onset. At all other times, we can compare the outputs of filter bank to the selected time. We have then multiple opinions on whether this time represents the same feature. As a way of combining these opinions into a single opinion, we use p-metrics. These are a parameterized class of distance functions in n-space. By using them to combine the opinions of the filters, we get what is essentially a fuzzy or, a fuzzy and, or something in between.

1.2. Onset Times

This study starts with a set of time series of neuromagnetic signals localized to some brain region. These contain evoked response waveforms time locked to a stimulus. The time lock is not perfect; there is “latency jitter,” i.e. variability in the time between the stimulus and the onset of the evoked response. Our primary goal is to measure the time of onset in individual trials.

Prior methods of calculating latency jitter have tended to use a template formed from an average ([5], [9], [14]). We instead incorporate expert knowledge by picking a sample trial. We are directly attempting to identify the leading edge of the waveform, and are not attempting to

align entire ERPs ([4]). Finally, we are not attempting to denoise the signal ([11], [12]). Rather we are teaching the computer to make comparisons between one time in the middle of a time series and another time in the middle of the same, or different, time series. We are focusing our efforts at teaching the computer to pick out points that represent the onset of an ERP, as this is perhaps the most important feature to measure.

1.3. Metrics from Filterbanks

Consider a discretized signal $s = s(t)$ and a linear filterbank F_1, \dots, F_n . A filter F_j gives us a real-valued function on the parameter space \mathbf{Z} , given by

$$s_j(t) = (F_j(s))(t).$$

This gives us a notion of distance on \mathbf{Z} namely the metric

$$d(t_1, t_2) = |s_j(t_1) - s_j(t_2)|.$$

This is the pull-back of the Euclidean metric on the real line by the function s_j .

This metric will be of limited utility. To improve on this, we consider the filterbank as a whole. At each time value we get a “feature vector” from which we typically want to derive a scalar that describes something of analytic value. We have a function \mathbf{F} from \mathbf{Z} to \mathbf{R}^n given by

$$\mathbf{F}(t) = (s_1(t), \dots, s_n(t)).$$

Given any metric δ on \mathbf{R}^n we have the pull-back metric d on \mathbf{Z} :

$$d(t_1, t_2) = \delta(\mathbf{F}(t_1), \mathbf{F}(t_2)).$$

This is a general scheme for deriving distance functions from filterbanks. In this study we use the distance functions to determine times that represent ERP onset.

1.4. Segmentation for Onset Detection

The waveforms that constitute the evoked response vary greatly in our data. We have no *a priori* knowledge of this waveform. One way to find the basic shape of this waveform is to use the average taken over all the trials, as in for example [11]. We take a different approach. We allow an expert to choose among the trials a “typical example” of an evoked response.

We treat onset detection as a segmentation problem. We need to separate within \mathbf{Z} values that represent the onset of an evoked response from those that do not. The sets we use to attempt such a segmentation are the unit balls

around a chosen t_0 for a varying pull-back metrics. That is we have a parameter space Γ and a metric δ_γ on n-space for each $\lambda \in \Gamma$. Let us denote the corresponding metric on time as $d_\gamma = \delta_{\mathbf{F}_\gamma}$. The set we use to try to define the onset points is then

$$\{t \in \mathbf{Z} \mid d_\gamma(t, t_0) < 1\}.$$

Because our data set is relatively small, we implemented an interactive system for varying γ and t_0 . This system was used to find onset detection better than in the previous study [8] on this data, as will be shown in the later sections.

1.5. Finding the Filterbanks

The success of the segmentation by metrics depends on the filterbank. We used multiresolution filterbanks that are one-dimensional analogs of the steerable filterbanks used in image analysis ([7]). The sizes of the kernels in the filters were adapted to each context—visual, auditory and somatosensory—by means of an interactive visualization system.

2. Time Series of Neuromagnetic Signals

The raw MEG time series were recorded by 122 sensors from human subjects performing either a simple sensory activation or cognitive tasks (for details see, [9]). Each experiment yielded a vector-valued time series $\mathbf{x} = \mathbf{x}(t)$.

2.1. SOBI recovered neuronal sources from MEG

Second order blind identification (SOBI) ([1], [2],[3]) a blind source separation algorithm (BSS) was applied to each \mathbf{x} , yielding an invertible matrix \mathbf{W} , called the unmixing matrix. The scalar components of $\hat{\mathbf{s}} = \mathbf{W}\mathbf{x}$ are maximally independent (in the statistical sense). These components are referred as recovered sources. Each recovered source has a corresponding field map giving information about the spatial location of the recovered source. The event-related potential (or stimulus triggered average) of each recovered source was examined to determine whether this recovered source was related to the processing of sensory stimulation. Those that were task-relevant and had source locations that were anatomically and physiologically meaningful were considered as neuronal sources ([9]).

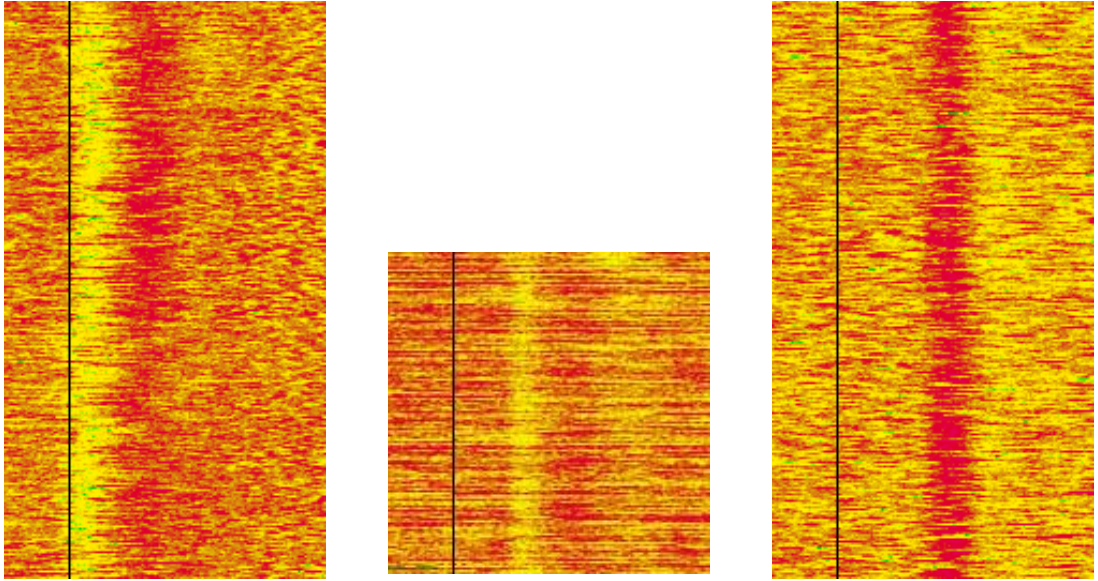


Figure 1. Single-trial evoked response potentials (ERPs) of SOBI recovered (left) somatosensory, (middle) auditory, and (right) visual sources.

2.2. Time Series of SOBI Recovered Sources

The present analysis solely focused on the temporal aspects of the SOBI recovered neuronal sources in three major sensory modalities: visual, auditory, and somatosensory systems. The inputs to the current study are the time series of SOBI recovered sources (Figure 1, reproduced from [8]), which have been shown to allow detection of response onset time in single-trials. Figure 1 shows examples of three time series from somatosensory, auditory, and visual SOBI components, shown as an MEG image—a pseudo-colored bit map in which each row represents one discrete trial of stimulation and multiple trials are ordered vertically from top to bottom. The time of the stimulation is indicated by the black vertical lines at time 0. The units in the vertical axis vary from one source to the next, and are irrelevant in this study, thus omitted in the figures. The time scales are identical, from -100 ms to 400 ms.

Although the signal to noise ratio via the SOBI pre-processing was improved in comparison to time series of MEG sensors, significant on-going background activity—an integral part of the neuronal source activation—remains in these derived time series (Figure 1). Such on-going activity can easily lead to false detection if a simple threshold method is used to measure evoked response onset time (see Table 1 for false detection rates from [8]). To reduce false detection rates, the proposed

multiresolution method was applied to the same time series of SOBI recovered neuronal sources.

3. Multiresolution ERP Onset Time Detection

3.1 Selection of the filterbank

Let \mathbf{s} denote one of the SOBI derived signals—a linear combination of the time series from the 122 sensors. Taking the linear combination, with the same coefficients, of the underlying continuous signals we get a derived signal f .

The discrete wavelet transform starts with a single waveform, or wavelet, ψ and scales and translates this waveform before taking the inner product with the signal. Thus the wavelet transform consists of the following scalars for each j and k :

$$\int_{-\infty}^{\infty} f(t)\psi(2^j t - k)dt$$

For these integrals to constitute a wavelet transform, technical conditions must hold on ψ . We don't need these conditions, so we ignore them. Thus we are doing multiresolution analysis, but not wavelet analysis.

In our filterbank, we allow for more than one waveform. We also allow more flexibility in the scaling and translations of the waveform. Thus we are computing the following integrals:

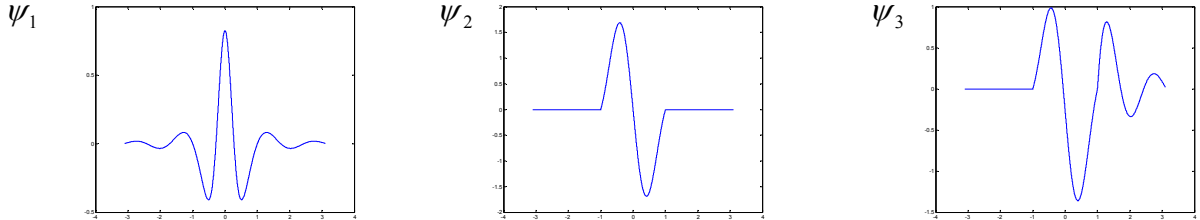


Figure 2. Waveforms for formula (1).

$$\int_{-\infty}^{\infty} f(t)\psi_l(\sigma t - \rho)dt. \quad (1)$$

Here we allow ψ_l to vary over three waveforms. The scales σ^{-1} vary over a small set not necessarily consisting of powers of two. The positions ρ vary over a set small enough to enable fast computation, but large enough to ensure that the resulting filterbank is a approximately shift invariant. For each l and σ we get a discrete signal as ρ varies. After resampling to the sampling rate of the discretized signal, we obtain the output of one of the linear filters in our filterbank.

The waveforms ψ_1, ψ_2 and ψ_3 are as shown in Figure 2. These were chosen in part to allow for code optimizations we will not discuss here. We do not believe their exact shapes are critical. The first waveform is fairly localized in frequency. The second is designed to pick up slope information. The third is asymmetric to be better at detecting the beginning of an ERP.

The scales σ^{-1} were chosen using an interactive visualization system to create outputs that carry equal amounts of information at each level.

3.2 Segmentation via Exemplars

We accomplish onset detection via segmentation into points that resemble a specific onset. We use an interactive system that shows the given time series and whatever segmentation the computer has derived. The user selects a point to represent onset and specifies parameters that determine the metric (distance function). The segmentation shown is the set of points deemed close to the exemplar point by the metric.

Consider a time series $s = s(t)$ and our filterbank F_1, \dots, F_n . Let $s_j(t) = (F_j(s))(t)$. The metrics

we use are

$$d(t_1, t_2) = \left(\sum w_j |s_j(t_1) - s_j(t_2)|^p \right)^{1/p}$$

where the weights w_j and the parameter p are to be determined by the user.

Typically more than one point near the start of an ERP will match sufficiently to be in the segmentation. Once we have heuristically selected a detection window, we define the onset time as the earliest point in that window that is a match preceded by a non-match. The false detections were defined in the same way, but in the pre- and post-control windows that are windows of the same duration immediately before and after the detection window.

4 The Results

4.1 Detection and False Detection

We compared the performance of the present method against results reported in a previous study [8] by applying the new method to the same sets of SOBI recovered neuronal sources.

In the previous study [8], onsets were calculated by looking for a threshold crossing after lowpass filtering. This is equivalent to using the present method, but with one filter. The new method examines signals at several frequencies, and thus is expected to do better at discriminating an ERP from background on-going activity. We found that to be the case (see Figure 4 for examples). For all three sensory modalities explored, the detection rates were significantly increased while the false-detection rate significantly decreased in comparison to previous findings (Table 1). For every single time series of SOBI recovered neuronal sources from a total of 10 subjects, the detection rate was increased and false detection rate was reduced.

Table 1.

	Somatosensory (N=8)		Visual (N=12)		Auditory (N=5)		Overall (N=25)	
	Detection	False Detection	Detection	False Detection	Detection	False Detection	Detection	False Detection
Previous	78 ± 2%	27 ± 4%	71 ± 2%	27 ± 3%	80 ± 6%	21 ± 3%	75 ± 2%	26 ± 2%
Current	87 ± 2%	16 ± 3%	77 ± 2%	13 ± 2%	89 ± 3%	6 ± 2%	83 ± 2%	13 ± 2%

4.2 Single-trial ERP Onset Times

Figure 3 shows three examples of detected single-trial ERPs for the somatosensory, auditory, and visual modalities. The black curve marks the detected onset time. The trials are sorted by the detected onset time, with the trials in which an ERP was not detected placed at the bottom. It is apparent that the detected onset times match to front edge of the single-trial ERPs. As a preliminary validation, we calculated a new average ERP by aligning each trial according to the detected onset time. If the estimated times are reasonable, this latency-corrected average should be sharper than the standard average. We found this to be the case for visual and somatosensory ERPs but not the auditory ERPs (Figure 4). The latter is not unexpected as in this data, we found little onset jitter in the auditory sources.

5 Discussion.

We introduced a novel method for detecting the onsets of single-trial ERPs by treating this problem as a one dimensional analog of image analysis. This method was implemented as an interactive software system which can be trained to find special points in an ERP or any other interesting waveforms. It offers a way to transform fuzzy expert knowledge into mathematical formulas. Thus, to use this system, the user need not understand the underlying mathematics. One the knowledge is transformed, the resulting mathematical formula can be used for future processing. The multiresolution metrics are fast to compute, making the system actually usable. This new method avoids the traditional template matching and the need to use average ERPs as templates.

Future work includes the generation of synthetic data to test the validity of the onset times calculated. We intend to modify some of the techniques in [5], [10], [11] and [14] to allow for direct comparative results.

Finally, we expect our methods to generalize easily to EEG data.

Acknowledgements

This work was supported by a DARPA grant to TAL and by DARPA and MIND Institute grants to ACT.

References

- [1] A. Belouchrani, K. A. Meraim, J.-F. Cardoso, and E. Moulines, "Second-order blind separation of correlated sources," in Proceedings International Conference on Digital Signal Processing, Cyprus, pp. 346-351, 1993.
- [2] A. Belouchrani, K. Abed-Meraim, J.F. Cardoso and E. Moulines, "A blind source separation technique using second order statistics", IEEE Trans. on Signal Processing, vol. 45, no. 2, pp. 434-444, 1997.
- [3] A. Belouchrani and J-F. Cardoso, "Maximum likelihood source separation by the expectation-maximization technique: deterministic and stochastic implementation", Proc. International Symposium on Nonlinear Theory and its Applications, Nolta'95.
- [4] L. Gupta, D. L. Molfese, R. Tammana, P. G. Simos, "Nonlinear alignment and averaging for estimating the evoked potential," IEEE Trans Biomed Eng. Vol. 43, No. 4, pp. 348-56, 1996.
- [5] P. Jaskowski, and R. Verleger, "Amplitudes and latencies of single-trial ERP's estimated by a maximum-likelihood method," IEEE Trans. Biomed. Eng. Vol. 46, pp. 987-993, 1999.
- [6] G. Salton, E. A. Fox, and H. Wu, "Extended boolean information retrieval," Communications of the ACM, Vol. 26, No 11, pp. 1022-1036, 1983.

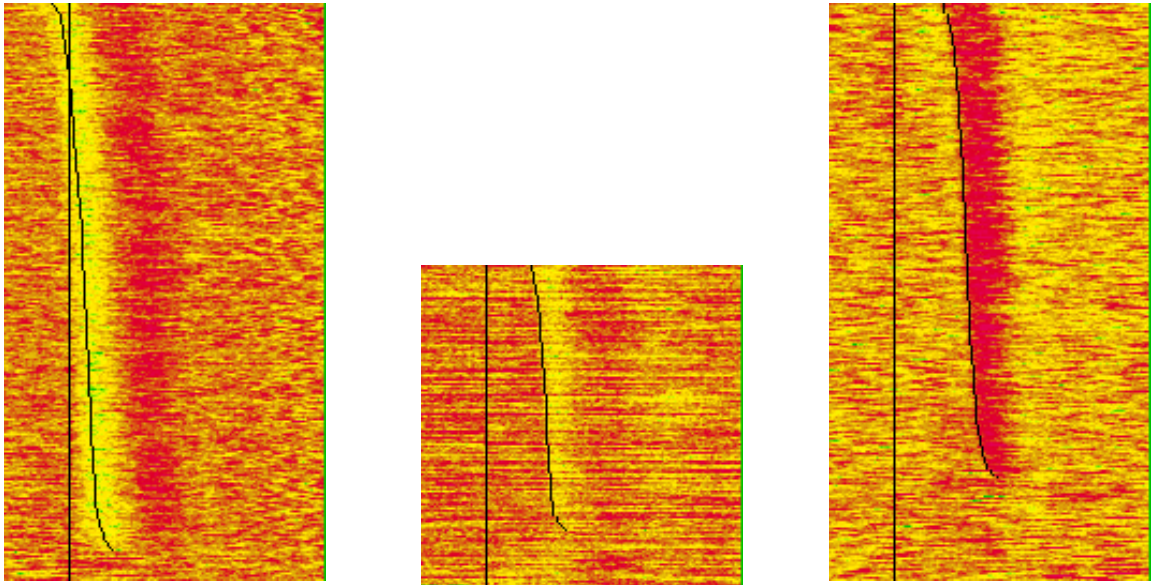


Figure 3. Examples of onset detection of single-trial evoked response potentials (ERPs) of SOBI recovered (left) somatosensory, (middle) auditory, and (right) visual sources.

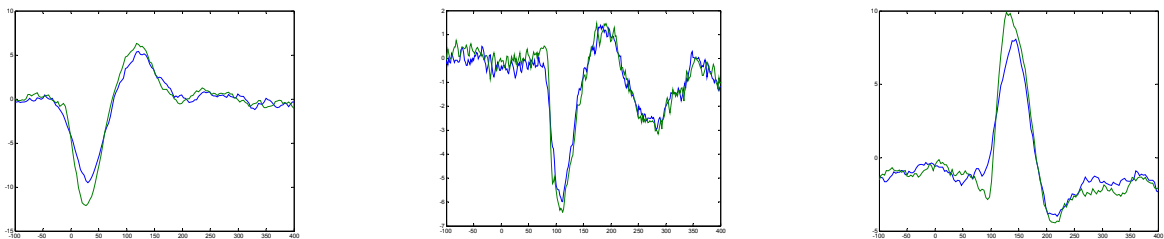


Figure 4. Average ERPs before (blue) and after (green) alignment according to the detected onset time. Left: somatosensory; middle: auditory; right: visual.

- [7] E. P. Simoncelli, W. T. Freeman, E. H. Adelson and D. J. Heeger, "Shiftable multi-scale transforms," *IEEE Transactions on Information Theory*, Vol. 38, pp. 587-607, 1992.
- [8] Akaysha C. Tang, Barak A. Pearlmutter, Natalie A. Malaszenko, and Dan B. Phung, "Independent components of magnetoencephalography: single-trial response onset time estimation," *NeuroImage*, Vol. 17, pp. 1773-1789, 2002.
- [9] Akaysha C. Tang, Barak A. Pearlmutter, Natalie A. Malaszenko, Dan B. Phung and Bethany C. Reeb, "Independent Components of Magnetoencephalography: Localization," *Neural Computation*, Vol 14 No 8, pp. 1827-1858, 2002.
- [10] D. Pham, J. Mocks, W. Kohler, and T. Gasser, "Variable latencies of noisy signals: Estimation and testing in brain potential data," *Biometrika* Vol. 74, p. 525, 1987.
- [11] R. Quian Quiroga, "Obtaining single trial evoked potentials with wavelet denoising," *Physica D*. Vol 145, pp. 278-292, 2000.
- [12] R. Quian Quiroga and E. L. J. M. Van Luijelaar, "Habituation and sensitization in rat auditory evoked potentials: A single-trial analysis with wavelet denoising," *International Journal of Psychophysiology*, Vol. 43, No 2, pp. 141-153, 2002.
- [13] Gilbert Strang and Truong Nguyen, *Wavelets and Filter Banks*, Cambridge Press, Wellesley, 1996.
- [14] C. Woody, "Characterization of an adaptive filter for the analysis of variable latency neuroelectric signals," *Med. Biol. Eng.* Vol. 5, pp. 539-553, 1967.